Swirling Flows between Coaxial Cylinders with Injection by Radial Jets

J.D. McLean* and E.H. Dowell†
Princeton University, Princeton, N.J.

An experimental program has been carried out to investigate a class of flows which is of interest with regard to the aeroelastic flutter of flexible cylinders. The flowfield of interest is the swirling flow between two concentric cylinders, of which the inner one is stationary and the outer one rotates. Air is admitted into the annulus between the cylinders through inlets in the wall of the rotating outer cylinder near one end of the apparatus and is exhausted through an annular outlet surrounding the inner cylinder near the other end. Measurements of the resulting flowfield have been made for a wide range of flow rates, outer cylinder rotational speeds, and inlet geometries. Approximate scaling laws for the velocity field have been developed, and dimensionless parameters have been defined which correlate the effects of the various inlet conditions which were tested.

Nomenclature

A_{an} = cross-sectional area of annulus
A_n = total cross-sectional area of inlets
d = internal diameter of inlet tubes
f = inner cylinder structural frequency
ℓ = length of inlet tubes
$\dot{m}$ = mass flow, lbm/sec
$\hat{M}$ = dimensionless momentum flux quantity, Eq. (4)
N = number of inlets
p, p_t = static pressure, pitot pressure
r = radius from cylinder axis
R_i = radius of inner cylinder (outside)
R_o = radius of outer cylinder (inside)
$\bar{R}$ = dimensionless radius $= (r-R_i)/(R_o-R_i)$
$\hat{t}$ = dimensionless "residence time" quantity, Eq. (5)
U_m = average axial velocity in the annulus $= \dot{m}/\rho A_{an}$
V = magnitude of fluid velocity
V_n = average radial velocity in inlets $= \dot{m}/\rho A_n$
V_t = tangential component of fluid velocity
V_z = axial component of fluid velocity
z = axial coordinate
β = yaw angle
Δ = pitot pressure referenced to the static pressure at the inner cylinder $= p_t - p(R_i)$
Γ = $V_t r$, circulation
Γ_o = ωR_o^2, (ideal) circulation at outer cylinder
ω = angular velocity of outer cylinder

I. Introduction

THE aeroelastic stability of cylindrical shells has been the subject of numerous investigations. Most of this effort has been concentrated on the problem of a cylindrical shell exposed to an external or internal fluid flow in the axial direction. However, another type of flow, in which the primary fluid motion is circumferential rather than axial, is important in some applications. For example, jet engines of dual-spool configuration produce swirling flows between rotating parts. Reported here are the results of an experimental investigation of a type of swirling flowfield which is effective in inducing flutter of cylindrical shell structures. A drawing of the experimental apparatus, which was designed to model the essential flowfield features occurring in one practical application, is shown in Fig. 1. The basic configuration consists of two coaxial cylindrical shells in which the inner cylinder is fixed and the outer cylinder rotates at high speed. Air is drawn in radially through several inlet holes or tubes around the circumference near one end of the outer cylinder and is exhausted at the other end through a central outlet surrounding the inner cylinder. The flow which is responsible for the flutter problem occurs in the annular region between the cylinders. Some combinations of inlet geometry and inlet flow rate can produce a vortex-like flowfield with large tangential velocities, which can be quite effective in inducing the flutter of a flexible inner cylinder.

This type of flutter belongs to a broad class of problems usually grouped under the name "panel flutter," or more formally, the "aeroelastic stability of plates and shells" (see Ref. 1 for a review of the literature). The basic physical phenomenon is the dynamic aeroelastic instability of a thin plate or shell structure due to the mutual interaction of the structural motion and the surrounding fluid flow. Flutter occurs when the mean flow velocity exceeds a critical value, known as the flutter velocity. The unusual feature of the present problem is the nature of the flowfield. The structure is conventional, a cylindrical shell, and the flutter of such structures has already been studied when the basic flow fluid is one of uniform velocity along the cylinder axis. However, in the present problem the flow is of a swirling, circumferential type, induced by the rotation of the outer cylinder.

In the first theoretical analysis of this flutter problem by Srinivasan,[3] the simplifying assumption of a potential model for the flowfield was made, which is conventional in aeroelastic work. The results of subsequent experimental work[4-6] showed that the quantitative accuracy of the potential flow theory was only fair and that a more general theoretical model, making use of a more detailed knowledge of the flowfield, would be required for accurate predictions of flutter behavior. The theoretical model was, therefore, extended by David and Srinivasan[7] to accept an arbitrary mean velocity profile as an input, and the experimental program described in the present paper was undertaken to provide the necessary detailed knowledge of the flowfield over a wide range of operating conditions.

The unique feature of the swirling flows investigated here is the manner in which the fluid enters the annulus. The flow through the inlets results in a mean radial flow in the region of the annulus immediately under the inlets. The effects of mean radial flow have been dealt with in the work of other in-

Received August 29, 1974; revision received May 9, 1975. This work was supported by Pratt and Whitney Aircraft, Division of United Aircraft Corporation. The authors would like to thank: J. B. Cooper, E. L. Griffith, G. Hazen, M. Hibbs, W. James, J. P. Kukon, W. F. Putman, J. J. Traybar, and C. S. Ventres of Princeton University; and K. Brown, C. Platt, and A. V. Srinivasan, of Pratt and Whitney.

Index categories: Subsonic and Transonic Flow; Aeroelasticity and Hydroelasticity.

*Member of Research Staff. Presently with Boeing Commercial Airplane Company, Renton, Wash.

†Professor, Department of Aerospace and Mechanical Sciences. Member AIAA.

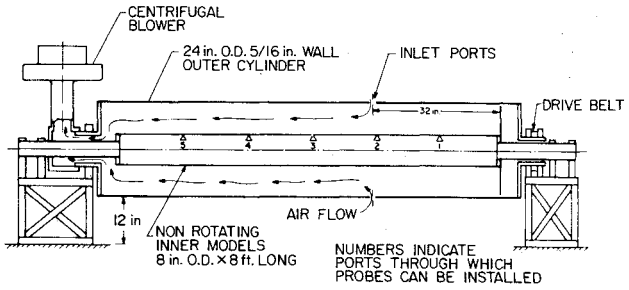

Fig. 1 Experimental apparatus.

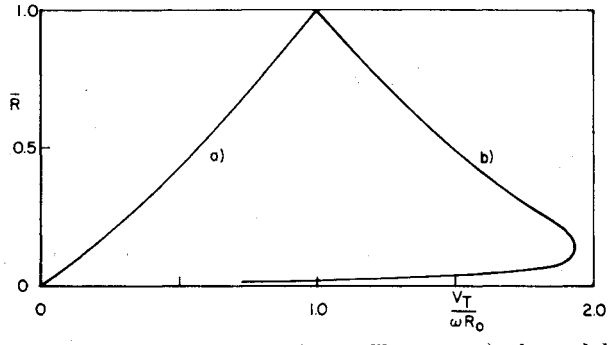

Fig. 2 Sketch illustrating velocity profile types: a) observed by Taylor (no radial flow); b) vortex-like flow produced by radial jets.

vestigators, but there are important distinctions to be made between the various ways in which radial flow can be introduced. Flows reported thus far in the literature represent two basic types of injection: Injection through a rotating porous outer cylinder, as in flows investigated by Pengelley[8] and Farris et al.,[9] or injection through tangential blowing jets in a stationary outer cylinder, as investigated by Donaldson and Snedeker[10] and Kendall.[11] In the present experimental apparatus the flow is introduced radially through small, discrete nozzles, forming radial jets of considerable intensity. The flux of radial momentum that these jets represent and the turbulence that they generate have important effects on the momentum transfer and the velocity profiles in the entire annulus. Such effects of inwardly directed radial jets in initiating a swirling flow have not been investigated previously, to the authors' knowledge.

Physical Nature of the Flowfield

Referring again to Fig. 1, three factors are expected to determine the flowfield in the annulus: the outer cylinder angular velocity ω, the detailed configuration of the inlets in the outer cylinder, and the flow rate through the inlets. Several inlet configurations were tested, varying both the number of inlets and their detailed geometry. Flow rates through the inlets were relatively small, so that the average axial velocity in the annulus downstream was considerably smaller than the tangential velocity of the outer cylinder, and as a result, the tangential component of velocity was the dominant one throughout most of the region of interest. The peripheral speeds of the outer cylinder ($\leq$200 fps) insured that the flow everywhere could be characterized as essentially incompressible.

In the process of establishing the velocity field in the entire annulus, interactions which occur in the region immediately under the inlets exert a dominant influence. In this region the mean radial velocity and the turbulence produced by the inlet jets have important effects on the momentum transfer and the resulting tangential velocity profiles and, as a result of these effects, the flow in the entire inlet region is jet-like in many of its features.

A pertinent property of turbulent jets is the dominance of the momentum flux as the primary quantity characterizing the mean velocity field. As a consequence, the radial momentum flux of the flow through the inlets is an important physical quantity characterizing the flow in the inlet region. Because the structure of turbulent freejets is relatively independent of Reynolds number, the mean velocity profiles produced by the jets in the inlet region do not vary strongly with Reynolds number. It follows from this jet-like behavior that the most useful dimensionless quantities for characterizing the flow are geometric and kinematic in nature rather than dynamic, and that the various Reynolds numbers which can be defined for the flow are of secondary importance. Thus, in terms of nondimensionalized velocity profiles, an approximate geometric similarity can exist between flows for which the inlet geometry and the appropriately nondimensionalized volume flow rate through the system are the same. For many of the combinations tested, for example, the profile of $V_t/\omega R_o$ was found to be nearly universal for a given inlet geometry and a given value of $U_m/\omega R_o$.

The region downstream of the inlets is quite different from the region directly under the inlets. This annular region between the inlets and the downstream exhaust port is characterized by a moderately high axial length-to-gap ratio, resulting in small radial velocities and forcing the flow to become quasi-cylindrical in nature. The resulting flow tends to be nearly uniform in the axial direction as a result of the balance between radial pressure gradient and centrifugal force which must exist in flows dominated by swirl (see Greenspan[12]).

Because this downstream region contains no mechanism adequate to maintain the turbulence introduced by the inlet jets, it seems reasonable to expect that the flow in this region will be the result of a compromise between the aforementioned tendency to remain uniform in the axial direction and a counteracting tendency to relax to a less energetic form. If the through-flow and the resulting jets were not present, the flow would assume the form observed by Taylor[13] between a rotating outer cylinder and a stationary inner cylinder. In this case the radial velocity gradient has a stabilizing effect on the turbulence, and the effective viscosity remains relatively low. The resulting tangential velocity profile is not much different from the corresponding profile in laminar flow (see Fig. 2). In the region of the inlets with the jets present, however, the jets tend to produce tangential velocity profiles which are nearly irrotational (like a potential vortex) except in a boundary-layer-like region near the inner cylinder (see Fig. 2). The detailed form of these profiles depends on the radial momentum flux and the inlet geometry, both of which affect the degree of tangential spin-up‡ achieved by the flow passing through the inlets. Since fluid with the velocity distribution produced by the inlet flow is convected downstream by the mean axial flow (and because of the quasi-cylindrical nature of the flow) the profiles produced in the inlet region tend to persist, changing only slowly, for the entire length of the downstream region.

II. Experimental Measurements

The general dimensions of the rotating cylinder apparatus are shown in Fig. 1. The outer cylinder drive system allows close control of the rpm. The airflow through the system is driven by an Allison supercharger, which permits up to 1 lbm/sec mass flow. The supercharger exhausts into a settling chamber, which in turn exhausts to the atmosphere through a converging nozzle, the minimum area of which was carefully measured. The dynamic pressure at the nozzle exit is monitored to obtain the volume flow rate through the system. The 8-in. o.d. thick-walled (¼ in) inner cylinder was equipped with six probe access ports at the locations shown.

Exploratory measurements with a rake of pitot-static tubes[14] indicated that flows which had produced flutter

‡Spin-up is a qualitative term indicating the magnitude and relative variation of the tangential circulation, $\Gamma \cdot \Gamma/\Gamma_o \rightarrow 1$ for all r would be termed complete spin-up.

during the flutter tests usually possessed peaks in tangential velocity near the inner cylinder. Because of this, subsequent detailed surveys of the flowfield concentrated only on the inner 3 in. of the annulus. A small pitot tube, flanked by two bevel-tipped yaw tubes (Fig. 3), was traversed radially through this region, beginning with the probe tip in contact with the inner cylinder wall. The pressure difference between the yaw tubes was monitored, and the yaw angle of the probe was continuously varied so as to keep the probe tip aimed into the local flow at every point in the traverse. The procedure is described in detail in Ref. 14. The reference pressure was provided by a nearby static pressure tap in the inner cylinder.

The method of obtaining velocity profiles from pitot-tube measurements is analogous to that used by Taylor[13] and is based on the approximate form of the radial momentum equation which results from the quasi-cylindrical approximation.[15] Near the inner cylinder of the present apparatus the conditions of the approximation are satisfied, with the exception of the region directly under the inlets. The approximate momentum equation is

$$\rho V_t^2/r = \partial p/\partial r \tag{1}$$

The local velocity, pitot pressure, and static pressure are assumed to be related by Bernoulli's equation

$$p_t - p = \tfrac{1}{2}\rho V^2 = \tfrac{1}{2}\rho(V_t^2 + V_z^2) \tag{2}$$

where $V_t = V\cos\beta$, and β is the local yaw angle. Combining Eqs. (1) and (2) and solving the resulting differential equation yields the square of the velocity as a function of radius. If the difference between the local pitot pressure and the static pressure at the inner cylinder is Δ, then

$$\Delta = p_t(r) - p(R_i)$$

and

$$V^2(r) = \frac{2}{\rho}\left[\Delta(r) - e^{-a(r)} \int_{R_i}^{r} \Delta(r') \frac{2\cos^2\beta(r')}{r'} e^{a(r')}\,dr'\right] \tag{3}$$

where

$$a(r) \equiv \int_{R_i}^{r} \frac{2\cos^2\beta(r')}{r'}\,dr'$$

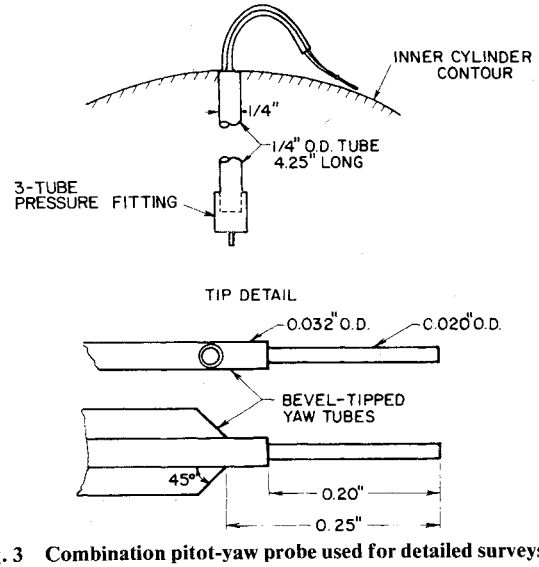

Fig. 3 Combination pitot-yaw probe used for detailed surveys.

Table 1 Inlet geometry combinations

Type of port	Number of ports	Diameter	Length	Probe station	RPM
Plain port	8	2″	5/16″	2	900
				3	900
				4	900
External tube	4	1″	5/8″	3	900
External tube	8	1″	5/8″	3	450
				3	900
External tube	8	1″	2″	3	450
External tube	4	1″	4″	3	450
External tube	8	1″	4″	2	450
				2	900
				3	450
				3	900
				4	450
				4	900
External tube	2	2″	1¼″	3	900
External tube	4	2″	1¼″	3	900
External tube	8	2″	1¼″	3	900
Internal tube	8	1″	2″	3	450
Internal tube	8	1″	4″	3	450

Thus, to obtain a velocity profile, the required data are the experimentally measured distributions $\beta(r)$ and $\Delta(r)$, where $\Delta(r)$ must be measured with the probe aligned with the local flow. A digital computer program was used to perform the integrations of Eq. (3) and to calculate profiles of tangential and axial velocity.

Most of the measurements were made at station 3, some measurements were made for two representative inlet geometries at station 4, and a few measurements were made at station 2. For each of the combinations of inlet geometry, probe location, and rpm, measurements were usually made at four different mass-flow rates. The combinations for which detailed profiles were measured are listed in Table 1, and the inlet nozzle geometries used are shown in Fig. 4.

III. Discussion of Results

Measured velocity profiles for all of the previous combinations of conditions are presented in Ref. 14. In the flows which produced flutter[5] the tangential velocity component was by far the dominant one. Thus, only the tangential velocity profiles will be discussed in detail here. Some notable features of these profiles are:

1) For many combinations the velocity profiles display an approximate similarity. Profiles measured at different rotational speeds with the same inlet geometry and at the same value of $U_m/\omega R_o$ generally fall close to a single curve (independent of ω). The profiles for $U_m/\omega R_o = 0.04$ in Fig. 5 are typical of the flows exhibiting this approximate similarity. Deviations from similarity are greatest at low relative flow

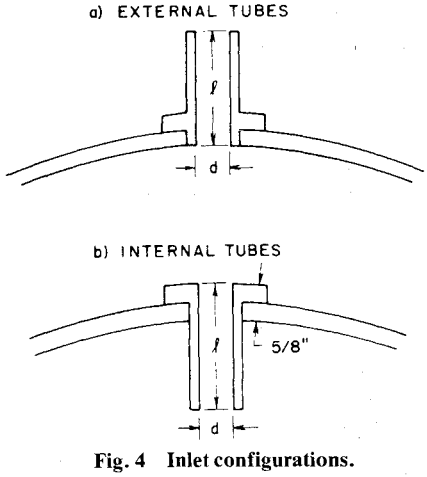

Fig. 4 Inlet configurations.

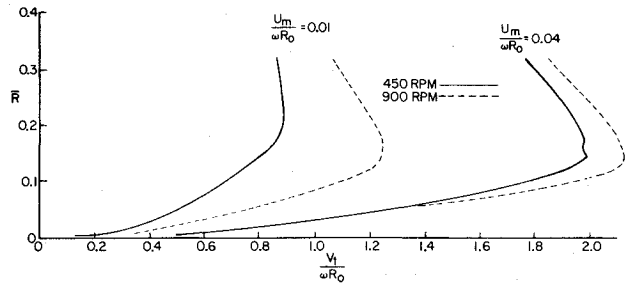

Fig. 5 Tangential velocity profiles at station 3; 8-1 in. × 4 in. external tubes.

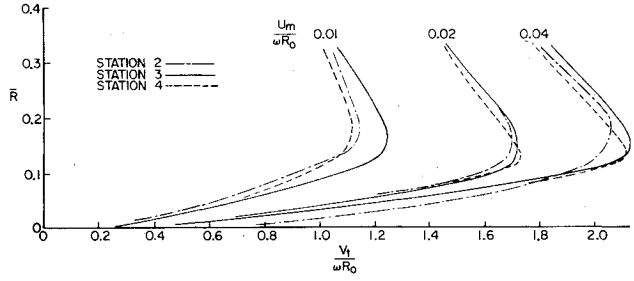

Fig. 6 Tangential velocity profiles at 900 rpm; 8-1 in. × 4 in. external tubes.

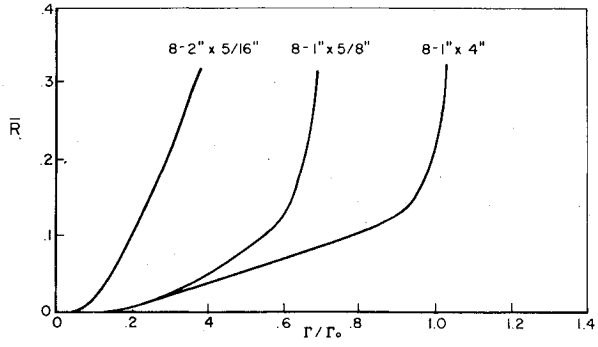

Fig. 7 Profiles of Γ/Γ_o at station 3; 900 rpm for different inlet configurations with $Um/\omega R_o = 0.04$.

rates, where the jets have less influence in establishing the profile and where Reynolds number is therefore more important (e.g., for $U_m/\omega R_o = 0.01$ in Fig. 5).

2) The changes in the profiles between the different axial stations are small, especially between stations 3 and 4 (see Fig. 6).

3) With all inlet geometries other than the 2-in. diameter ports, high relative flow rates produce vortex-like flows in which the velocity increases toward the center, except in a boundary-layer-like region surrounding the inner cylinder.

The degree to which the different flows are vortex-like can be illustrated by plotting the dimensionless circulation $\Gamma/\Gamma_o = V_t r/\omega R_o^2 \cong Vr/\omega R_o^2$. The profile of Γ/Γ_o in a potential vortex would be constant with radius. Plots of Γ/Γ_o for typical cases at a high relative flow rate are shown in Fig. 7. The profile for the 8-2 × 5/16-in.[§] inlet configuration is not vortex-like at all. In this case, the inlets are so short in the radial direction that a high degree of spin-up is not achieved by the air passing through the ports. The large inlet area results in a relatively low radial momentum flux for a given mass-flow rate, and the resulting turbulent mixing is not as strong as it would be with smaller diameter ports. By way of contrast, the outer portion of the profile produced by the 8-1 × 4-in. inlet configuration is quite vortex-like, Γ/Γ_o being nearly constant at a value of 1.0. In this case, the long tubes result in almost perfect spin-up, and the momentum flux is sufficient to produce a nearly irrotational profile. The profile produced by the 8-1 × 5/8-in. configuration is also vortex-like, with Γ/Γ_o nearly constant at around 0.7 in the outer portion. Here, the shorter tubes result in less than perfect spin-up, but a vortex-like profile is still produced.

These profiles illustrate the importance of two factors in determining the form of the tangential velocity profile: 1) The radial momentum flux at the inlets is important in determining the degree to which the profile is vortex-like (irrotational) in its outer portion; 2) The length of the inlet tubes is important in determining the degree of spin-up achieved by the inlet flow. Dimensionless variables expressing a quantitative measure of each of these factors can be defined, and it has been found that an appropriate choice of such variables can provide a useful approximate correlation of some important features of the velocity profiles.

To characterize the radial momentum flux at the inlets, a dimensionless momentum flux quantity $\hat{M}$ is defined

$$\hat{M} \equiv V_n^2 A_n/\omega^2 R_o^2 A_{an} = (U_m/\omega R_o)^2 A_{an}/A_n \quad (4)$$

where V_n is the radial velocity averaged over the cross-sectional area of the inlets. To characterize the effect of the inlet tube length in determining the degree of spin-up, the velocity V_n and the length of the inlet tubes can be used to define an average residence time of an air particle in the inlet tube. The ratio of the average residence time to the time required for the inlet tube to move one diameter tangentially provides the definition of a dimensionless residence time

$$\hat{t} \equiv (\ell/V_n)/(d/\omega R_o) = [(\ell/d)/(U_m/\omega R_o)](A_n/A_{an}) \quad (5)$$

Certain important features of the tangential velocity profiles have been found to correlate reasonably well with the quantities $\hat{M}$ and $\hat{t}$; and thus these two quantities may be used in combination to provide an approximate prediction of the type of flow which will result from a given inlet geometry and mass flux. In flows possessing a peak in the velocity profile, the maximum tangential velocity was also found to correlate well with $\hat{M}$ and $\hat{t}$. This correlation of $(V_t\text{max})/\omega R_o$ with $\hat{M}$ and $\hat{t}$ is shown in Fig. 8, where values of $(V_t\text{max})/\omega R_o$ are given in a log-log plot of $\hat{t}$ vs $\hat{M}$.¶ Here particular inlet geometries represent straight lines, since

$$\hat{t} = \ell/d(A_n/A_{an})^{1/2}\hat{M}^{-1/2} \quad (6)$$

Equation (6) expresses the fact that $\hat{t}$ decreases as $\hat{M}$ increases for a fixed inlet geometry. This decrease in the residence time as $\hat{M}$ is increased provides a plausible explanation of why for some inlet geometries (those toward the bottom of Fig. 8) $(V_t\text{max})\omega R_o$ first increase and then decrease as $\hat{M}$ is increased.

The correlation of Fig. 8 is reasonably close. In places where values for more than one case occupy the same $(\hat{M}, \hat{t})$ point on the plot, the scatter is generally considerably smaller than the variation of $(V_t\text{max})/\omega R_o$ over the whole plot. By cross-plotting values from Fig. 8, it was possible to construct contours of approximately constant $(V_t\text{max})/\omega R_o$, as shown in Fig. 9.

The contours of Fig. 9 illustrate the unexpected result that increasing the length of the inlet tubes (increasing $\hat{t}$) at a con-

§Hereafter, a shorthand notation is adopted for describing inlet geometries. For example, the description "8 − 1 × 4-in. inlets" refers to the inlet configuration consisting of 8 tubes of 1-in. diameter and 4 in. length. Tubes are assumed to be external (Fig. 4a) unless described otherwise.

¶This correlation is intended to apply only to external tube configurations, for which the bulk of the measurements were made. Internal tube configurations were included in the plot by redefining R_O as the radial location of the inner ends of the inlet tubes, in effect treating them as external tubes mounted in a smaller outer cylinder. Even with this adjustment, it is not expected that the correlation will work as well for internal tubes as it does for external tubes.

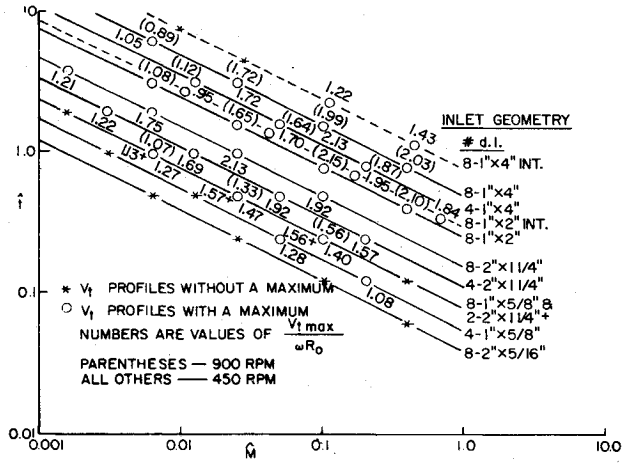

Fig. 8 $(V_t\text{max})/\omega R_0$ as a function of $\hat{M}$ and $\hat{t}$.

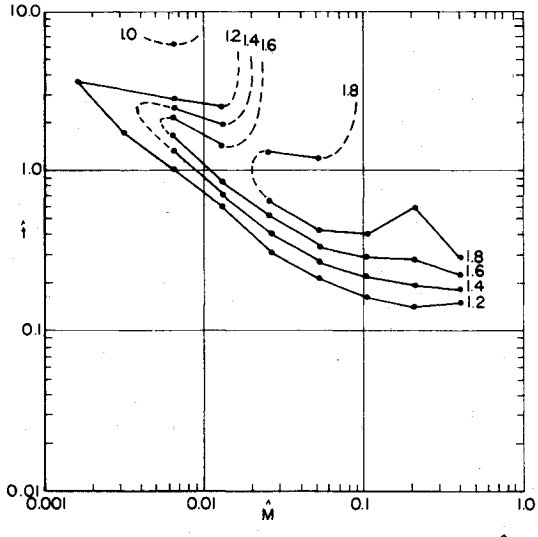

Fig. 9 Contours of constant $(V_t\text{ max})/\omega R_0$ in terms of $\hat{M}$ and $\hat{t}$.

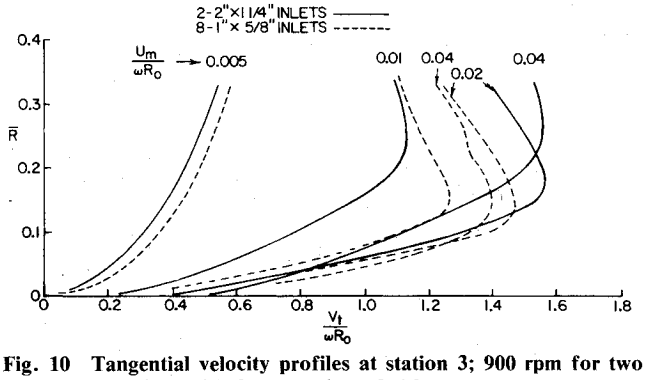

Fig. 10 Tangential velocity profiles at station 3; 900 rpm for two inlet configurations with the same A_n and ℓ/d.

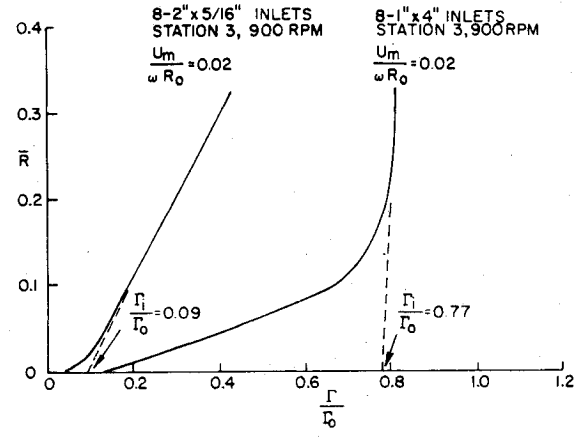

Fig. 11 Illustrating the definition of Γ_i/Γ_0.

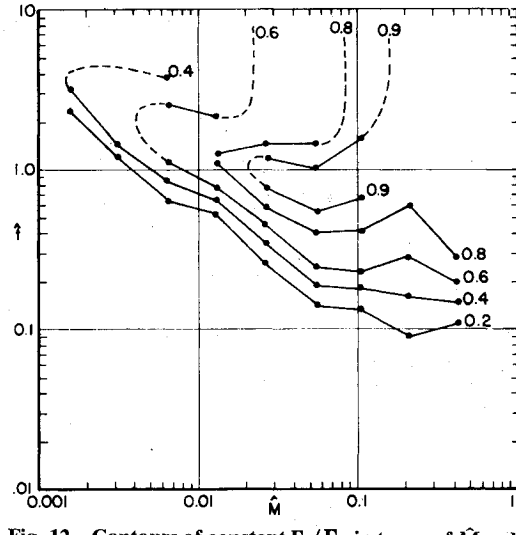

Fig. 12 Contours of constant Γ_i/Γ_0 in terms of $\hat{M}$ and $\hat{t}$.

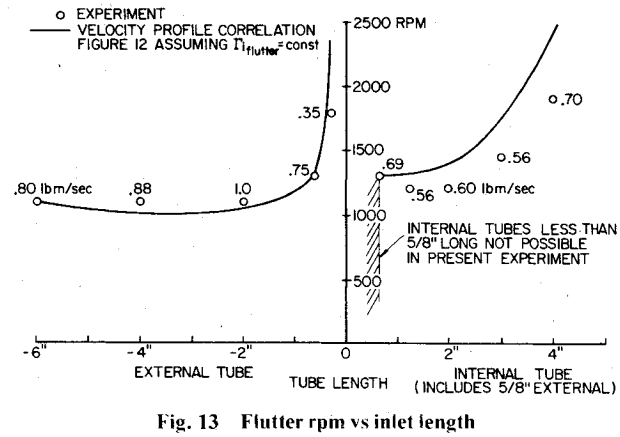

Fig. 13 Flutter rpm vs inlet length

stant value of $\hat{M}$ does not always produce a monotonic increase in $(V_t\text{max})/\omega R_o$. At values of $\hat{M}$ below 0.013, increasing $\hat{t}$ first produces an increase in $(V_t\text{max})$ and then a decrease. The initial increase is due to the increased spin-up achieved as the inlets are lengthened. But after the spin-up is increased beyond a certain point, the momentum flux apparently becomes increasingly inadequate to produce a vortex-like profile at the higher velocity associated with the high spin-up, and $(V_t\text{max})$ then decreases.

The correlation of Fig. 9 implies a rather simplified physical picture in which the total cross-sectional area of the inlets and their length to diameter ratio ℓ/d determine the form of the velocity profile for a given $U_m/\omega R_o$ regardless of the number of inlets. In Fig. 10 profiles are compared for the 2-2×1¼-in. inlet configuration and the 8-1×5/8-in. configuration, where both configurations have the same A_n and ℓ/d. At given values of $U_m/\omega R_o$, the maximum velocities produced by the two configurations are similar, but the profiles are not identical. At $U_m/\omega R_o = 0.01$ the eight-inlet configuration appears to produce more vigorous mixing, as indicated by the higher peak velocity occurring closer to the wall, but at $U_m/\omega R_o = 0.02$ and 0.04 the two inlet configuration produces greater spin-up.

In spite of the simplification it represents, the correlation of Fig. 9 is close enough to provide approximate predictions of

peak tangential velocities. The peak velocity by itself, however, did not prove to be an accurate indicator of the miminum outer cylinder speed required to produce flutter. As the result of a search for a single feature of the velocity profile which would correlate reasonably well with the flutter data of Ref. 6, a consistently definable feature of the Γ/Γ_0 profile has been found which also correlates reasonably well with $\hat{M}$ and $\hat{t}$. As shown in Fig. 11, the outer portion of the profile measured in the detailed survey is extrapolated to the inner cylinder wall, defining a quantity Γ_i/Γ_0. In Fig. 11 this is shown for both a vortex-like profile and a nonvortex-like profile. The correlation of Γ_i/Γ_0 corresponding to Figs. 8 and 9 was found to be reasonably good, and the resulting contours are shown in Fig. 12. This correlation, like the one for $(V_t \text{ max})/\omega R_0$, can serve as a useful guide as to the type of velocity profile that will be produced by a given inlet geometry. Moreover, under the assumption that a given inner cylinder will flutter at a fixed value of Γ_i, it can be used to predict the effect of changes in inlet geometry on the minimum flutter speed. To use Fig. 12 in this way, the minimum flutter speed and mass flow must be known for one inlet geometry. From this known flutter condition the corresponding values of $\hat{M}$ and $\hat{t}$ are calculated, and the corresponding value of Γ_i/Γ_o is read from Fig. 12 and denoted by $\Gamma_{i(\text{flutter})}$. The procedure for predicting the minimum flutter speed for other inlet geometries consists of using Fig. 12 to find the minimum speed which will give this value of Γ_i for each new geometry. This is done by finding on Fig. 12 the maximum value of Γ_i/Γ_o which is consistent with each new inlet geometry and taking the minimum outer cylinder speed required for flutter to be given by

$$\Gamma_0 = \Gamma_{i(\text{flutter})} / (\Gamma_i/\Gamma_0)_{\max}$$

This prediction procedure has been tested against the flutter data of Ref. 6 for an 8-in. diameter, 0.020-in. wall, aluminum outer cylinder. The 8-1 × 5/8-in. inlet configuration was used as the reference, and Fig. 13 shows the resulting predictions for 1-in. diameter inlets of other lengths. The procedure works fairly well except for the 4-in. internal tubes, where the velocity correlation of Fig. 12 did not work too well. Unfortunately, this prediction doesn't work for the 2-in. diameter port data (flutter rpm predicted is too high by a factor of four or so), indicating the Γ_i is only a reasonable indicator of flutter in cases where the velocity profile is reasonably vortex-like. For the nonvortex-like profiles produced by 2-in. diameter ports, the situation is evidently more complicated, and a more complete theory, one responsive to the complete mean velocity field, will be required.

The theory described recently by David and Srinivasan[7] represents a step in this direction, and the data presented here can provide a basis for evaluating its predictions. Because the results of the present measurements were not yet available to them, David and Srinivasan used the results of preliminary measurements reported in Ref. 14 as the input to their theory. Because these preliminary measurements did not provide details of the profile near the inner cylinder, David and Srinivasan carried out calculations for several plausible extensions of the measured profile, which they showed in Fig. 4 of Ref. 7. Of these postulated inner region velocity profiles, the one most nearly resembling the results of the present measurements ($V_1^s/b\Omega_2 = 0.6$ in the notation of Ref. 7) leads to a predicted flutter speed of about 2300 rpm (see Fig. 5 of Ref. 7). The measured velocity profile used for this prediction corresponds to the 8-1 × 5/8-in. inlet configuration, for which the measured flutter speed was aobut 1400** rpm. The earlier version of the theory,[3,6] in which a potential flow velocity profile was assumed, predicted a flutter speed of 780 rpm for this case. Thus, where the simple theory predicted too low a flutter speed, the more complete theory predicts too high a speed. It appears that, if accurate flutter speed predictions are to be made, further refinement of the theoretical model will be required.

**Apparently due to a misunderstanding, David and Srinivasan incorrectly attributed the measured velocity profile shown in their Fig. 4 to the 8-1 × 5/16-in. inlet configuration, for which the measured flutter speed was 1800 rpm.

IV. Conclusions

The experimental program described here and in more detail in Ref. 14 has provided a general physical understanding of the flowfield in the annulus. The radial momentum flux through the inlets and the inlet length to diameter ratio were found to be important factors determining the nature of the velocity field. Dimensionless parameters have been postulated which provide a reasonably good quantitative correlation of these effects, and approximate scaling laws for the velocity field have been established. The latter have been used successfully to predict the variation of flutter velocity with inlet geometry for vortex-like flows. For flows which are not vortex-like, the theoretical approach used by David and Srinivasan shows promise, but further refinement will be required.

References

[1] Dowell, E. H., *Aeroelasticity of Plates and Shells*, Noordhoff International Pub., Leyden, The Netherlands, 1974.

[2] Paidoussis, M. P., "Dynamics of Cylindrical Structures Subjected to Axial Flow," *Journal of Sound and Vibration*, Vol. 29, Aug. 1973, pp. 365-385.

[3] Srinivasan, A. V., "Flutter Analysis of Rotating Cylindrical Shells Immersed in a Circular Helical Flowfield of Air," *AIAA Journal*, Vol. 9, March 1971, pp. 394-400. Also see Part II, AIAA Paper 71-373, Anaheim, Calif., 1971.

[4] Dowell, E. H., Griffith, E. L., Ambrose, J. G., and Ventres, C. S., "Experimental Study of the Flutter of a Flexible Cylinder due to a Rotational, Swirling Flow," Princeton Univ. AMS Rept. 1039, April 1972, Princeton, N.J.

[5] Ambrose, J. G., "Flutter of a Cylindrical Shell in a Swirling Flow," presented at *Symposium on Aeroelasticity of Turbomachines*, Indianapolis, Ind., June 1-2, 1972.

[6] Dowell, E. H., Srinivasan, A. V., McLean, J. D., and Ambrose, J. G., "Aeroelastic Stability of Cylindrical Shells Subjected to a Rotating Flow," *AIAA Journal*, Vol. 12, Dec. 1974, pp. 1644-1652.

[7] David, T. S. and Srinivasan, A. V., "Flutter of Coaxial Cylindrical Shells in an Incompressible Axisymmetric Flow," *AIAA Journal*, Vol. 12, Dec. 1974, pp. 1631-1635.

[8] Pengelley, C. D., "Flow in a Viscous Vortex," *Journal of Applied Physics*, Vol. 28, Jan. 1957, pp. 86-92.

[9] Farris, G. J., Kidd, G. J., Jr., Lick, D. W., and Textor, R. E., "Theoretical and Experimental Study of Confined Vortex Flow," *Journal of Applied Mechanics*, Vol. 36, Dec. 1969, pp. 687-692.

[10] Donaldson, C., DuP. and Snedeker, R. S., "Experimental Investigation of the Structure of Vortices in Simple Cylindrical Vortex Chambers," Aeronautical Research Associates of Princeton Rept. 47, Dec. 1962, Princeton, N.J.

[11] Kendall, J. M., "Experimental Study of a Compressible Viscous Vortex," Jet Propulsion Laboratory Technical Rept. 32-290, 1962, Pasadena, Calif.

[12] Greenspan, H. P., *Theory of Rotating Fluids*, Cambridge Univ. Press, Cambridge, 1969.

[13] Taylor, G. I., "Fluid Friction between Rotating Cylinders II—Distribution of Velocity between Concentric Cylinders When Outer One is Rotating and Inner One Is at Rest," *Proceedings of Royal Society of London*, A Vol. 157, Dec. 1936, pp. 565-578.

[14] McLean, J. D. and Dowell, E. H., "Experimental Study of the Flutter of a Flexible Cylinder due to Swirling Flow. Part II: Flowfield Investigation and Additional Flutter Tests," Princeton Univ., AMS Rept. 1039, Nov. 1973, Princeton, N.J.

[15] Hall, M. G., "Structure of Confined Vortex Cores," *Progress in Aeronautical Sciences*, Vol. 7, Pergamon, New York, 1966.